Journal of Materials Chemistry B

Accepted Manuscript

ROYAL SOCIETY OF CHEMISTRY

www.rsc.org/materialsB

Journal of
Materials Chemistry B

RSCPublishing

Paper

Facile preparation of cancer-specific polyelectrolyte nanogels from natural and synthetic sugar polymers

Cite this: DOI: 10.1039/xoxx00000x

Received ooth January 2012,
Accepted ooth January 2012

DOI: 10.1039/xoxx00000x

www.rsc.org/

Fang Yuan,[a] Shasha Wang,[a] Wei Lu,[b] Gaojian Chen,[*b] Kehua Tu,[a] Hongliang Jiang[a] and Li-Qun Wang[*a]

Glyco-nanogels are glycopolymer-decorated nanoparticles of three-dimensional cross-linked networks, which have attracted ever-increasing interest of biomedical-related community. However, most of current reported glycosylated nanogels are prepared by copolymerization of glycopolymers with co-monomers and cross-linkers. Physically self-assembled glyco-nanogels remain a big challenge and are rarely explored. Herein, we report a new synthesis of glycosylated polyelectrolyte nanogels (glyco/CS nanogels), which are self-assembled from glycopolymer (PMAG-*b*-PMAA) synthesized through reversible addition-fragmentation chain transfer polymerization (RAFT) and quaternary ammonium chitosan (QACS) via electrostatic interactions under physiological conditions (pH 7.4, NaCl 0.15 M). The resultant glyco-nanogels had been demonstrated very stable in 10 mM HEPES buffer solution at least for 7 days and a specific binding capability to Con A. Their structure composed of an ionically cross-linked core and glucose corona was confirmed by TEM. Compared with normal cells, glyco/CS nanogels exhibited a much higher affinity and cytotoxicity towards K562 cancer cells. In addition, the cellular uptake of these nanogels by K562 was further imaged via fluorescent microscopy in which nanogels with yellow-green signals were found to eventually co-locate within the cell nuclei of K562. The incorporation of natural and synthetic sugar polymers into polyelectrolytes has provided an insight to easily prepare glyco-nanogels with excellent colloidal stability, specific bioactivities and imaging ability, suggesting their great potential for biomedical applications.

1. Introduction

Carbohydrates are important bioactive ligands involved in pivotal biological events, such as specific cellular recognition and cell signalling.[1, 2] They can interact with receptors on cell surfaces[3, 4] and recognise lectins, mainly for 'multivalent effect' employed in biological systems.[5-7] Recently, nanoparticles with glycopolymers surfaces (glyco-NPs) have attracted widespread attention due to their potential biomedical applications.[8-10] This is because their glycosylated surfaces can not only enhance the colloidal stability of nanoparticles, but also possess unique bioactivities.

Diverse glyco-NPs have been prepared by various approaches. For example, glyco-NPs can be prepared via grafting glycopolymers onto hydrophobic matrixes,[11-16] or from core-shell micelles formed by sugar-related amphiphilic polymers.[17-23] Amongst them, glyco-nanogels are glyco-NPs with three-dimensional cross-linked networks. In general, nanogels can be fabricated by chemical synthesis or physical methods.[24] Many chemically prepared glyco-nanogels have been prepared by copolymerization of glycopolymers with co-monomers and cross-linkers.[25-30] However, physically self-assembled glyco-nanogels remain a big challenge and are still rarely explored.

Polyelectrolyte nanogels, which are readily formed via electrostatic interactions between two oppositely charged polyelectrolytes, have a booming development in bio-applications over the last decade.[31-33] Compared with chemically cross-linked nanogels, physically prepared nanogels possess superior advantages with respect to their biomedical application because of a milder preparation condition without using toxic cross-linker, catalyst and by-product. However, the electrostatic interactions of polyelectrolyte complexes are usually too weak to survive under complex physiological conditions, such as high salt concentration and dilution in vivo. In order to overcome these drawbacks, polyion copolymers containing poly (ethylene glycol) (PEG) are used to form block ionomer complexes[34-38] with good colloidal stability owing to excellent steric effect of PEG coating. Nevertheless, PEGylation is also known to decrease bioactivity of PEGylated protein,[39] and low transfection efficiency of lipoplexes,[40-42] etc., thereby PEG remains controversial for some biomedical fields[43, 44]. Glycopolymers, by contrast, can be a good alternative for PEG. They exhibit excellent biocompatibility and provide some unique bioactivity for bio-applications, not just a stabilizer like PEG. For example, Deng et al prepared monodisperse and stable glyco-NPs via electrostatic interaction of glycose-derived cationic glycopolymers P(APMA)-*b*-P(GAPMA) with DNA. Moreover, their

sugar moieties were proved to be highly efficient for gene delivery.[45] Kurtulus et al developed a endosomal escaping agent P(AEAEMA)-*b*-P(ManAc) containing a spermine-like block and a mannose block. These block polymers were able to complex with DNA and provide cell-recognition ability to the polyplex particles.[46]

In this work, we report novel glycosylated polyelectrolyte nanogels (glyco/CS-nanogels) formed by block ionomer complexes between synthetic glycopolymers and quaternary ammonium chitosan (QACS). Firstly, well-defined hydrophilic-block-anionic glycopolymers (PMAG-*b*-PMAA) were synthesized via a RAFT polymerization. Then, the electrostatic self-assembly behaviours between the PMAG-*b*-PMAA and QACS with different molecular weight (MW) and their titration order were comprehensively investigated. Under optimal condition, glyco/CS-nanogels with compact ionic cross-linking core and glucose corona were obtained and showed a good colloidal stability in 10 mM HEPES buffer solution (pH 7.4, NaCl 0.15 M). These nanogels exhibited specific binding ability to lectin (Con A) because of inspired 'multivalent effect' of glucose corona. Compared with normal cells, higher polycation-induced cytotoxicity of glyco/CS-nanogels towards K562 cancer cells was observed due to their glucose corona's strong affinity towards glucose transporters (GLUTs) which are over-expressed in most cancer cells[47-50]. Additionally, the imaging ability of these nanogels was evaluated. The glyco/CS-nanogels are very promising for potential biomedical applications owing to their specific bioactivities together with good imaging ability.

2. Experimental section

2.1 Materials

Quaternary ammonium derivatives of middle viscosity chitosan (QACS 1, degree of substitution (DS) = 55.6%) and degradable chitosan (QACS 2, DS = 59.4%) were prepared and characterized according to our previous work[51] (Scheme 2b), with $M_{n(GPC)}$ values of 560 362 and 22 838 g mol^{-1}, respectively. 2-Cyanoprop-2-yl-α-dithionaphthalate (CPDN) was synthesized and characterized according to a previously reported method.[52] 2, 2'-Azobis (isobutyronitrile) (AIBN) (Aladdin, 98%) was recrystallized three times from ethanol. Methacrylic acid (MAA, stabilized with MEHQ) (TCI, 99%) was passed through a column of activated neutral alumina before use. Methacryloyl chloride (stabilized with MEHQ) (TCI, 80%), D-(+)-glucosamine hydrochloride (TCI, 98%), fluorescein *o*-acrylate (FA) (Aldrich, 95%), hexylamine (Aldrich, 99%), Con A from *Canavalia ensiformis* (Jack bean) (Sigma, typeVI, lyophilized powder), PNA from *Arachis hypogaea* (peanut) (Sigma, lyophilized powder, affinity-pureified), BSA (Sinopharm Chemical Regent Co., Ltd., BR), and DAPI (Invitrogen) were used directly as received. 10 mM HEPES buffer solution (pH 7.4, containing 0.15 M NaCl, 1 mM Ca^{2+}, and 0.01 mM Mn^{2+}) was used as solvent to prepare polyelectrolyte solutions. All other solvents (Sinopharm Chemical Regent Co., Ltd., AR) were used as received without further purification.

2.2 Synthesis

Synthesis of 2-(methacrylamido) glucopyranose (MAG). The MAG monomer was prepared as described previously.[18] Briefly, glucosamine hydrochloride (5.0 g, 2.32 × 10^{-2} mol) and potassium carbonate (3.2 g, 2.32 × 10^{-2} mol) were dissolved in 250 mL of methanol in a 500 mL single neck round-bottom flask with vigorously stirring. The mixture was later cooled down to -10 °C using a methanol/ice bath before methacryloyl chloride (2.25 mL, 2.32 × 10^{-2} mol) was dropwise added into the mixture. The mixture was stirred at -10 °C for 30 min and left to react for 3 h at room temperature. The crude mixture was filtered through a sintered funnel under vacuum to remove precipitated salts, and the filtrate was concentrated under reduced pressure to give off-white slurry. The slurry was purified by a column chromatography with dichloromethane/methanol (ratio 4:1) as the eluent. The white solid exited the column with the R_f value of 0.33, with a yield of 50% obtained gravimetrically. ^{1}H NMR (400 MHz, D_2O, ppm): 5.69 (s, 1H, Me-C=C*H*H), 5.46 (s, 1H, Me-C=CH*H*), 5.21-5.22 (d, 0.6H, anomeric α-CH), 4.76-4.78 (d, 0.4H, anomeric β-CH), 3.42-3.96 (m, 6H, sugar moiety's 4×CH and 1×CH_2), 1.92 (s, 3H, CH_3).

Homopolymerization of MAG with CPDN (PMAG Macro-CTA). Typically, MAG (1.0 g, 4.05 × 10^{-3} mol), AIBN (3.32 mg, 2.02 × 10^{-5} mol) and CPDN (21.9 mg, 8.08 × 10^{-5} mol) and solvent *N*, *N*-dimethylacetamide (DMAc, 4 mL) were added to a dry glass ampule with a magnetic bar. The ampule was sealed after bubbled with argon for 1 h, and then the formed solution was stirred at 70 °C for 24 h. After that, the ampule was cooled with ice water and opened. The reaction mixture was precipitated into an excess of methanol. The final polymer was dialyzed (MWCO = 3500) against distilled water for 2 days to remove impurities, followed by lyophilisation to obtain a pink powder with a yield of 90%. ^{1}H NMR (400 MHz, D_2O, ppm): 7.52-8.24 (m, 7H, CH of naphthalene units), 5.0-5.33 (d, 1H, anomeric CH), 3.35-4.05 (m, 6H, sugar moiety's 4×CH and 1×CH_2), 1.72-1.85 (m, 2H, CH_2 of main chain), 0.8-1.1 (s, 3H, CH_3 of main chain) (^{1}H NMR spectrum of PMAG in DMSO-d_6 was also given in Fig. 1b).

Synthesis of anionic diblock glycopolymer (PMAG-*b*-PMAA) with PMAG Macro-CTA. Typically, MAA (0.2 mL, 2.36 × 10^{-3} mol), AIBN (0.97 mg, 5.90 × 10^{-6} mol) and PMAG Macro-CTA (297.6 mg, 2.36 × 10^{-5} mol) and solvent *N*, *N*-dimethylacetamide (DMF, 3 mL) were added to a dry glass ampule with a magnetic bar. The ampule was sealed after bubbled with argon for 1 h, then the formed solution was stirred at 70 °C for 24 h. The following steps were the same as those to prepare PMAG Macro-CTA described above. The final glycopolymer was obtained as very pale pink spongy solid with a yield of 64%. ^{1}H NMR (400 MHz, DMSO-d_6, ppm): 6.89-8.12 (m, 7H, CH of naphthalene units), 4.70-5.26 (d, 1H, anomeric CH), 2.81-3.98 (m, 6H, sugar moiety's 4×CH and 1×CH_2), 1.47-2.22 (m, 2H, CH_2 of PMAA moieties), 0.4-1.4 (m, 3H, CH_3 of PMAG-*b*-PMAA), 12-13 (m, 1H, COOH of PMAA moieties)

Fluorescent labeling of glycopolymer with fluorescein *o*-acrylate (PMAG-*b*-PMAA-FA). Glycopolymer was terminal tagged with FA via thiol-ene click chemistry. PMAG-*b*-PMAA (50 mg, 0.0033 mmol) and FA (1.26 mg, 0.0033 mmol) were dissolved in 3 mL of dry DMF and bubbled with argon. Then, hexylamine (0.86 μL, 0.0066 mmol) in 2 mL of dry DMF was added using a syringe. The reaction mixture was then stirred at 50 °C under argon for 24 h before dialyzed (MWCO = 3500) against distilled water for 5 days, followed by lyophilisation to afford final yellowish product.

Colloidal titration assay. PMAG-*b*-PMAA and QACS 1 (or 2) were dissolved in 10 mM HEPES buffer solution with a final concentration of 1 mg mL^{-1} for each polymer. Both of them were filtered through 0.45 μm filters prior to titration. Firstly, UV-Vis spectra of PMAG-*b*-PMAA and QACS were measured and 700 nm was determined as the work wavelength to eliminate the influence from absorbance (Abs) of materials. Typically, 3 mL QACS 1 (or 2) was taken as the starting solution of which transmittance (T%) was reset as 100%. Then solution of PMAG-*b*-PMAA was pipetted into the starting solution at a dose of 100 μL for each time and the mixture was stirred vigorously for 2min prior to T% measurement.

Preparation of glyco/CS-nanogels. Firstly, PMAG-*b*-PMAA and QACS 1 were dissolved in 10 mM HEPES buffer solution (pH 7.4, 10 mM) with a final concentration of 1 mg mL^{-1}, and were filtered through 0.45 μm membrane syringe filter prior to use. Then,

glyco/CS nanogels were prepared by adding varying volume of PMAG-*b*-PMAA into constant QACS 1 (3 mL). These complexes were stirred for 1 h, followed by standing overnight at room temperature prior to characterization.

2.3 WST-8 assay

The cell viability of the glyco/CS nanogels was evaluated by WST-8 (water soluble tetrazolium salts) assay using cell counting kit-8 (CCK-8, 7sea biotech). Briefly, 20 μL of RPMI medium 1640 (HyClone) containing K562 or Ba/F3 cells (within 5% recombinant murine IL-3, Peprotech.) were seeded in 96-well microtiter plates (1×10^4 cells per well) with 80μL of glyco/CS nanogels at various concentration. Untreated cells were used as the control. Then, both K562 and Ba/F3 cells were incubated at 37 °C in a 5% CO_2 atmosphere. After 24 h, 10 μL of CCK-8 reagent was added to each well, and then the cells were incubated for 4 h. After that, Abs (450 nm for soluble dye and 650 nm for viable cells) were measured using a microplate reader (Thermo Fisher Scientific Inc.). Data were presented as average ± SD (n = 6).

2.4 Characterization

The $M_{n(GPC)}$ and polydispersity index (PDI) of the polymers were estimated on a gel permeation chromatograph (GPC) consist of a Waters 1515 Isocratic HPLC Pump with Waters 2410 refractive index detector (RI). Samples were eluted using eluent composed of 70% NaH_2PO_3 (0.1 M) / $NaNO_3$ (0.2 M) buffer solution (pH 7) and 30% methanol through a Agilent PL aquagel-OH MIXED-M column at a flow rate of 1 mL min^{-1}. The $M_{n(GPC)}$ was determined relative to PEG standards. ^{1}H NMR measurements of the polymers were carried out on a Bruker DMX-400 nuclear magnetic resonance (NMR) instrument operating at 400 MHz, using D_2O and DMSO-d_6 as solvent. The fluorescence spectra were obtained on a Perkin Elmer LS55 luminescence spectrometer at E_x = 485 nm (E_x slit = E_m slit = 5.0 nm, scan speed = 50 nm min^{-1}, voltage = 800 V). Colloidal titration assay and turbidimetry assay were recorded on a Shimadzu (Kyoto, Japan) UV-1800 at 700 nm. Hydrodynamic diameter (D_h) and Zeta potential of glyco/CS nanogels were measured using dynamic light scattering (DLS) (Malvern nanoZS-90 size analyzer, UK). The morphology of these nanogels was observed with a JEOL JEM-1200EX transmission electron microscope (TEM) operating at an acceleration voltage of 80 kV. Samples were deposited from solutions of polyelectrolyte nanogels onto copper grids coated with carbon. Water was allowed to evaporate from the grids under air. Fluorescent microscopy images were examined using an IX71inverted research microscope (Olympus, Tokyo, Japan) equipped with a multiple fluorescent filter turret.

3. Results and discussion

3.1 Synthesis of PMAG and PMAG-*b*-PMAA by RAFT polymerization

In our study, PMAG-*b*-PMAA was obtained in two steps (1and 2 in Scheme 2a). Firstly, PMAG homopolymer (PMAG Macro-CTA) was synthesized via a RAFT polymerization using CPDN as the RAFT agent and AIBN as the initiator. Subsequently, the anionic diblock glycopolymer, PMAG-*b*-PMAA, was synthesized by RAFT polymerization using PMAG Macro-CTA as the RAFT agent. The GPC and NMR results of PMAG and PMAG-*b*-PMAA was shown in Fig. 1 and Table 1. As presented in Fig. 1a, well-defined PMAG (PDI = 1.22) and PMAG-*b*-PMAA (PDI = 1.36) were successfully obtained. The chemical structure of glycopolymer was confirmed by ^{1}H NMR spectra shown in Fig. 1b, with clear observation of the peaks corresponding to the aromatic protons of the CPDN units (δ = 6.89-8.12 ppm), the proton of carboxyl group on methacrylic acid (δ = 12~13 ppm), the proton of anomeric carbon (δ = 4.71~5.26 ppm) and other protons of sugar moieties (δ = 2.81-3.98 ppm). The molar ratio between MAG and MAA (n_{MAG} : n_{MAA}) was determined by the integral areas of protons on anomeric carbon and carboxyl group. The MW of glycopolymers calculated by NMR ($M_{n(NMR)}$) was found to be close to the theoretical ones ($M_{n(th)}$). However, it was noteworthy that the $M_{n(GPC)}$ values determined by GPC were not comparable with $M_{n(th)}$. They were only apparent values because PEG was used as the calibration standard for aqueous GPC measurement.

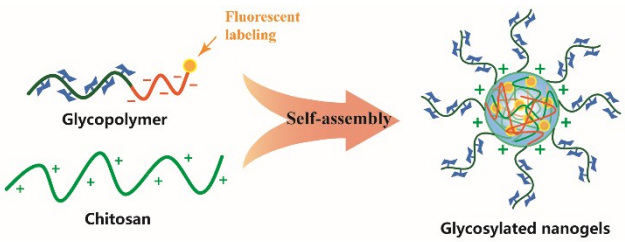

Scheme 1. Schematic illustration of the preparation of bioactive polyelectrolyte nanogels from natural and synthetic sugar polymers.

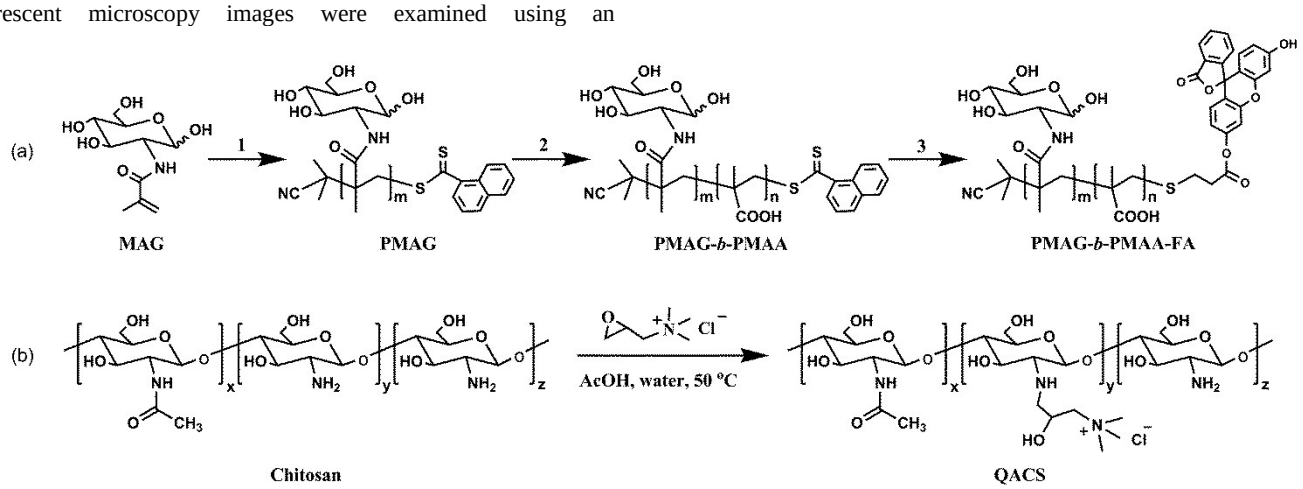

Scheme 2. Synthesis of (a) PMAG-*b*-PMAA and PMAG-*b*-PMAA-FA: (1) CPDN, AIBN, DMAc, 70 °C; (2) MAA, AIBN, DMF, 70 °C; (3) Hexylamine, FA, anhydrous DMF, 50 °C; and (b) Quaternary ammonium chitosan (QACS).

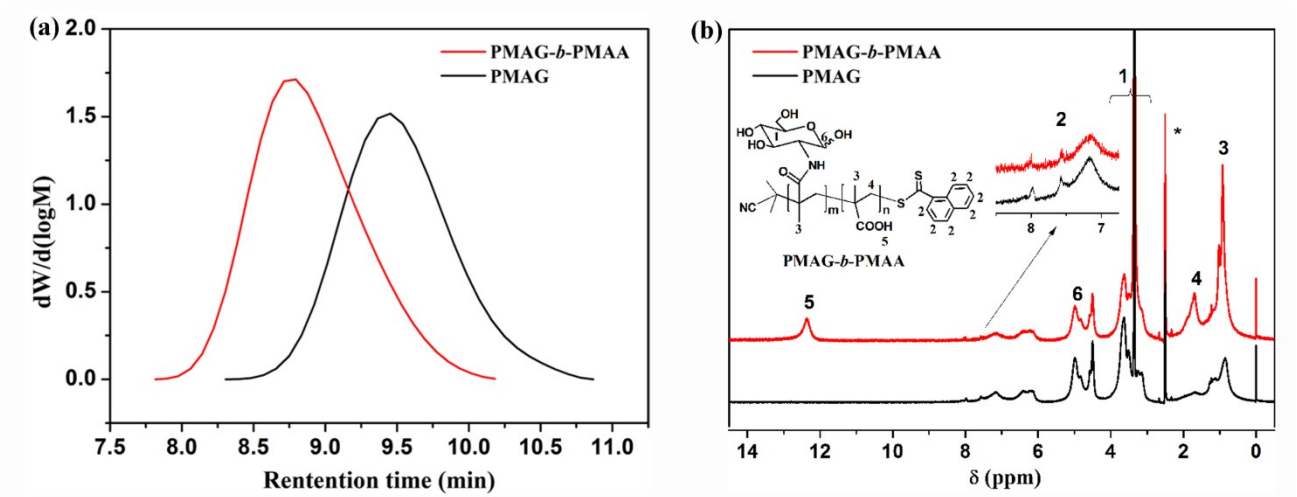

Fig. 1. (a) GPC traces and (b) ^{1}H NMR spectroscopy of PMAG and PMAG-*b*-PMAA (in DMSO-d_6).

Table 1. Characteristics of PMAG and PMAG-*b*-PMAA synthesized via RAFT polymerization.

Glycopolymers	Conversion [%]	$M_{n(th)}$ [g mol^{-1}]	$M_{n(NMR)}$ [g mol^{-1}]	$M_{n(GPC)}$ [g mol^{-1}]	PDI	n_{MAG}:n_{MAA}
PMAG	100%	12 600	14 100	3312	1.22	null
PMAG-*b*-PMAA	35%	21 200	17 100	9469	1.36	1.6:1

In addition, the presence of the dithioester groups in the terminal of PMAG-*b*-PMAA provided further scope for bio-imaging application via thiol-ene click chemistry. Herein, fluorescein *o*-acrylate (FA) labelled PMAG-*b*-PMAA (PMAG-*b*-PMAA-FA) was obtained using hexylamine as catalyst to reduce the dithioesters of PMAG-*b*- PMAA to thiols[53] and catalyse nucleophile-initiated thiol-michael reaction[54] with FA in one-pot (3 in Scheme 2a). Fluorescence emission spectra presented a broad emission band with λ_{max} of 512 nm for PMAG-*b*-PMAA-FA compared with unlabelled PMAG-*b*-PMAA (shown in Fig. S1), indicating the successful labelling with FA.

3.2 Formation and characterization of glyco/CS-nanogels in 10 mM HEPES buffer solution.

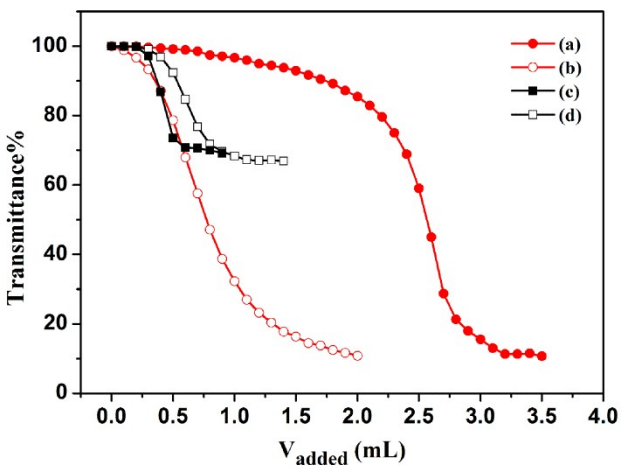

Fig. 2. Colloidal titration assay of PMAG-*b*-PMAA with QACS 1 (or 2) in 10 mM HEPES buffer solution (pH 7.4, NaCl 0.15 M): (a) starting: QACS 1, added: PMAG-*b*-PMAA; (b) starting: PMAG-*b*-PMAA, added: QACS 1; (c) starting: QACS 2, added: PMAG-*b*-PMAA; (d) starting: PMAG-*b*-PMAA, added: QACS 2. All the concentrations were 1 mg mL^{-1}.

The electrostatic self-assembly behaviours between QACS and PMAG-*b*-PMAA were investigated via colloidal titration assay. Herein, two kinds of QACS with different MW were involved. Due to a similar DS for QACS 1 and 2, the total charge density of them was almost equal when they are at the same concentration (1 mg mL^{-1}). In a colloidal titration assay curve, transmittance (T%) of the starting solution will continuously decrease after the oppositely charged component is added, due to the formation of polyelectrolyte complexes. In this study, a series of reverse S-shaped colloidal titration curves containing three stages were obtained. Generally, T% of the starting solution decreases gradually in stage 1, then sharply goes down in stage 2, finally reaches to a plateau in stage 3. We have previously shown that stable colloidal nanogels were always obtained in the "colloidal region" between stage 1 and early stage 2,[51] therefore a relatively long stage 1 is preferred. Amongst the four curves presented in Fig. 2, curve a and c start with QACS as the initial solution. Effective colloidal region was observed for curve a where PMAG-*b*-PMAA was added into QACS 1. This was because the higher MW of QACS 1 made that QACS 1 possessed a larger charge number per single chain than its shorter analogous QACS 2. After being neutralized with equivalent opposite charges (less than stoichiometric point), the chains of QACS 1 were able to possess much more residual positive charges to preserve the existing colloidal complexes from early aggregation. Meanwhile, due to high viscosity of QACS 1, the chain rearrangement of PMAG-*b*-PMAA/QACS 1 complexes was slowed down, helping to maintain the colloidal stability of complexes. Whereas, in the case that PMAG-*b*-PMAA was used as the starting solution (curve b and d), all added positive charges would be quickly neutralized by excess negative charges. Both the colloidal regions of curve b and d were almost negligible, indicating that the difference in MW of QACS could be ignored when they were added into PMAG-*b*-PMAA. In summary, the MW of QACS and titration order between PMAG-*b*-PMAA and QACS play an important role in the formation of stable colloidal nanogels.

Guided by results of colloidal titration assay, glyco/CS-nanogels with varying negative/positive (neg/pos) ratios were

formed by adding different volume of PMAG-*b*-PMAA into constant QACS 1 ($V_{QACS\ 1}$ = 3 mL). As shown in Fig. 3a, the D_h of glyco/CS-nanogels gradually increased from 172 nm to 283 nm as the neg/pos ratio changed from 0.1 to 0.45 (0.5 mL < $V_{PMAG\text{-}b\text{-}PMAA}$ < 2.25 mL). However, the D_h quickly increased over 500 nm accompanying with large aggregation when the neg/pos ratio came to 0.5 ($V_{PMAG\text{-}b\text{-}PMAA}$ = 2.5 mL). Combined with the result in Fig. 2, it was found that the nonlinear increase of D_h depended on the reversed S-type of curve a. Whereas, different from continuously increase of D_h, the PDI decreased firstly and then increased, with a minimum value at neg/pos ratio = 0.4 ($V_{PMAG\text{-}b\text{-}PMAA}$ = 2 mL). Fig. 3b showed the Zeta potential values of these nanogels. Interestingly, the Zeta potential increased gradually as the addition of PMAG-*b*-PMAA. It was different from those of polyelectrolyte nanogels formed by QACS 1 with citraconic-based *N*-(carboxyacyl) chitosan[51] which was a pure polyanion without a non-ionic hydrophilic moieties like PMAG. Herein, the presence of PMAG could possibly affects the electrostatic self assembly behaviour and chain rearrangement of glyco/CS-nanogels.

According to theories of block ionomer complexes, these glyco/CS-nanogels are apt to form nanoparticles containing an ionically cross-linked inner core and a glucose outer corona. As presented in Fig. 4a, the morphology of nanogels was confirmed by TEM. Gray halos around black cores were clearly viewed, which was highly possible the glucose corona. The distinct native contrast in TEM image is due to the different electron density between compact inner core and loose outer boundary. Fig. 4a inset showed the average diameter of glyco/CS-nanogels in aqueous solution was 228 nm with a narrow dispersity (PDI < 0.1). However, the dried nanogels in TEM image shrunk with an extent of 30%-60% because of evaporation of water.

To demonstrate the colloidal stability of glyco/CS-nanogels, we further monitored the changes of D_h and Zeta potential over time in 10 mM HEPES buffer solution (Fig. 4b). Results showed that the D_h and Zeta potential of glyco/CS-nanogels almost remained constant at least for 7 days, indicating their excellent colloidal stability under physiological condition. Moreover, these nanogels did not disintegrate even upon a 50 or 100-fold dilution from the initial concentration of 1 mg mL^{-1} (shown in Fig. S2). Such high colloidal stability of glyco/CS-nanogels even without chemical cross-linking is owe to the combination of efficient steric effect of glucose corona, electrostatic repulsion of excess positive charges and high viscosity of QACS 1.

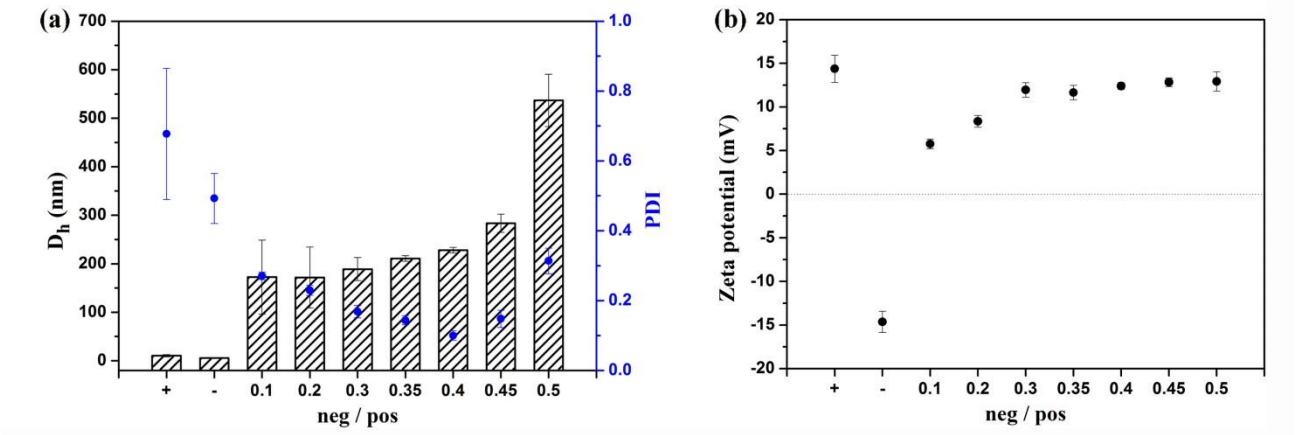

Fig. 3 (a) DLS and (b) Zeta potential values of glyco/CS-nanogels formed by adding PMAG-*b*-PMAA into QACS 1 with varying neg/pos ratio between negative and positive charges.

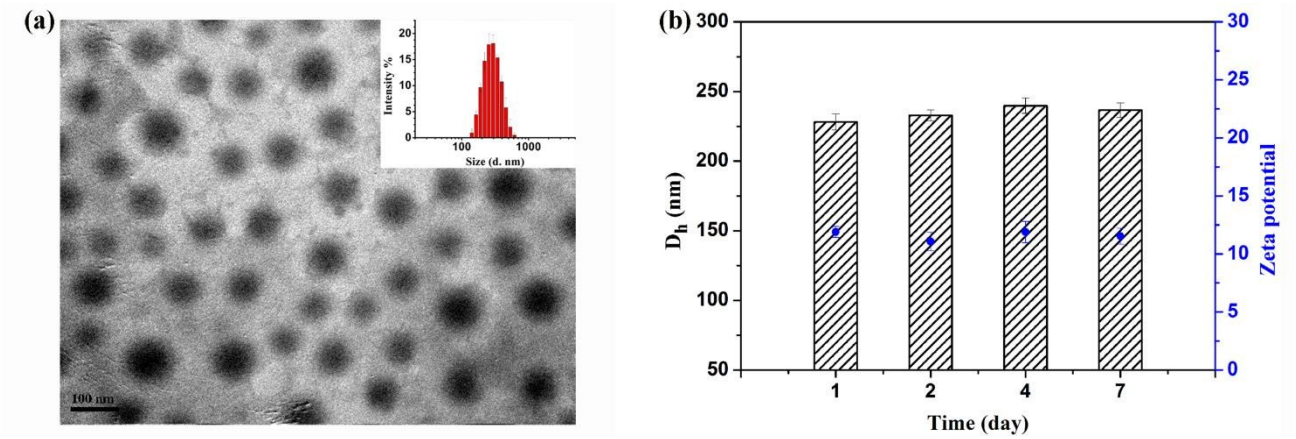

Fig. 4. (a) TEM image (scale bar = 100 nm) and size distribution (in the upper right inset) and (b) Colloidal stability over time of glyco/CS-nanogels (neg/pos ratio = 0.4) formed in 10 mM HEPES buffer solution (pH 7.4, NaCl 0.15 M).

Journal of
Materials Chemistry B

RSCPublishing

Paper

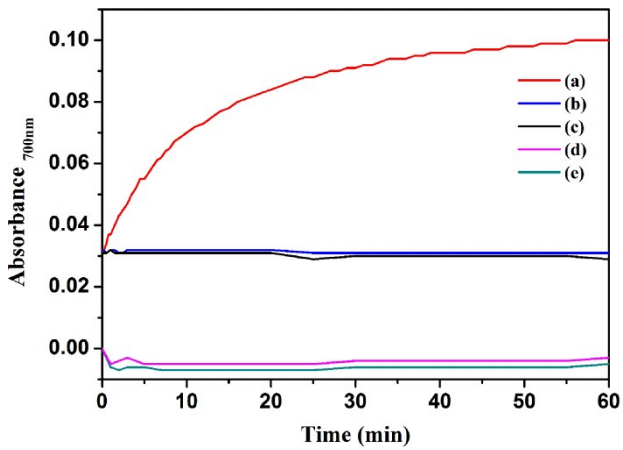

Fig. 5. Turbidimetry assay results (a) Lectin Con A, glyco/CS nanogels; (b) Lectin PNA, glyco/CS nanogels; (c) BSA, glyco/CS nanogels; (d) Lectin Con A, free QACS 1 with equivalent molarity as it is in glyco/CS nanogels; (e) Lectin Con A, free PMAG-*b*-PMAA with equivalent molarity as it is in glyco/CS nanogels. Concentration of Con A, PNA, BSA and glyco/CS nanogels were 1mg mL^{-1}.

3.3 Bioactivities of glyco/CS-nanogels.

Carbohydrates presented peculiar ability in biological recognition events mediated by a specific recognition process. To investigate the bioactivities of glyco/CS-nanogels, we firstly characterized their lectin-binding ability via turbidimetry assay. Briefly, we added glyco/CS-nanogels into Con A and monitored the change of Abs at 700 nm using UV-Vis spectrometer (Fig. 5). After 200 μL of glyco/CS-nanogels solution was added into 600 μL of Con A solution, the Abs of mixture solution instantaneously increased due to the intrinsic colloidal turbidity of glyco/CS-nanogels. Then, Abs quickly and continuously increased within 30 min, followed by reaching a plateau in 1 h. However, in a control experiment, Abs was unchanged when the nanogels were added into peanut agglutinin (PNA) that was selective binding of galactose, not glucose. These results indicated the specific binding ability of glyco/CS-nanogels to Con A. Whereas, it was noteworthy that the free PMAG-*b*-PMAA did not recognise Con A because the Abs was also unchanged except for a slight decline resulting from small dilution of the Con A solution. Our understanding is that the glycopolymers have a weaker binding ability with Con A compared to mannose-containing polymers. But their binding ability will be greatly enhanced due to the strong 'multivalent effect' which is

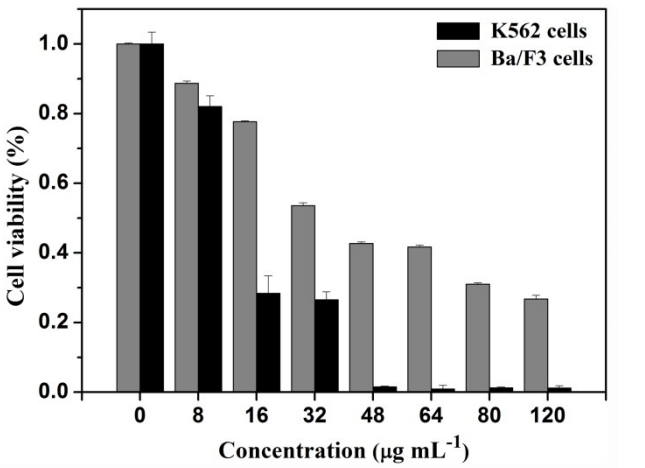

Fig. 6. WST-8 assay results of K562 and Ba/F3 cells treated with glyco/CS nanogels at various concentrations after incubation for 24 h.

displayed by gathering them on the boundary of nanogels. This is similar to those observations from other reported glycosylated micellar system[18, 55] which has a high sugar density arranged in a spherical shape. Additionally, free QACS 1 did not recognise Con A either. It was demonstrated that the binding of glyco/CS-nanogels to Con A was independent of charges and chitosan itself. In contrast, under certain conditions, glucose corona can obstruct the electrostatic binding of the cationic nanogels with some negative charged molecules, like protein BSA. Because the possible electrostatic interactions can be restrained by the steric effect of glucose corona.

To further test the high affinity of glyco/CS-nanogels towards cancer cells, K562 and normal bone marrow-derived murine pro-B-lymphocyte (Ba/F3) cells were chosen as a model. As leukemia cells, K562 cells over-express GLUTs, especially GLUT-1[56-58] that possesses high affinity towards glucose and glucosamine. Whereas, the level of GLUTs in Ba/F3 cells is relatively low. Fig. S3 showed that the nanogels could give rise to cellular apoptosis owing to the polycation-induced cytotoxicity. However, the glucose corona endowed these cationic nanogels with different affinity towards K562 and Ba/F3 cells. The effect of glyco/CS-nanogels on cell viabilities of the two cells lines were assessed via WST-8 assay. As shown in Fig. 6, glyco/CS-nanogels showed a higher cytotoxicity to K562 than Ba/F3 cells in all tested concentrations. Their higher cytotoxicity to K562 was associated with enhanced binding ability and increased cellular uptake by glucose corona. These natural and

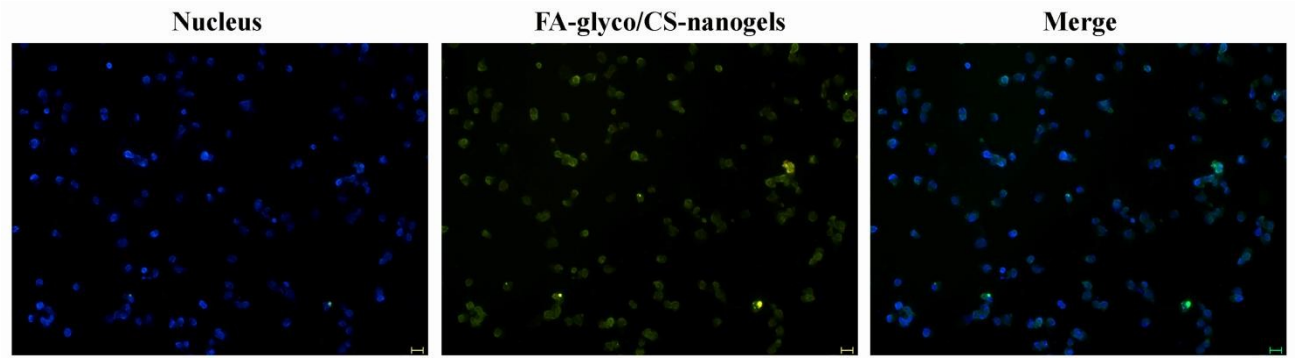

Fig. 7. Fluorescent microscopy images of K562 cells incubated with FA-glyco/CS-nanogels (48 μg mL^{-1}) for 6 h. Left: nucleus was stained by 0.5 μg mL^{-1} DAPI (blue); middle: FA-glyco/CS-nanogels (yellow-green); right: merge of fluorescence images. Scale bar = 20 μm.

synthetic sugar polymers incorporated nanogels have been demonstrated a great potential as an agentia free of encapsulating small molecular drug, which can be applied to cancer topical administration for effectively killing cancer cells.

The cellular uptake of glyco/CS-nanogels could be imaged by fluorescent microscopy using fluorescent nanogels (FA-glyco/CS-nanogels) composed of PMAG-*b*-PMAA-FA and QACS 1. Fig. 7 showed the fluorescent images after co-incubating K562 and FA-glyco/CS-nanogels for 6 h, where blue cell nuclei of K562 and yellow-green FA-glyco/CS-nanogels were respectively in the left and middle view. Furthermore, the fluorescent signals of nanogels were found to highly overlap with those of the cell nuclei according to the merge view. It suggested that FA-glyco/CS-nanogels could be internalized and finally bound with cell nuclei due to formation of conjugates between these cationic nanogels and phosphate groups of the DNA.

4. Conclusions

In summary, novel electrostatically self-assembled glyco-nanogels with glucose corona, composed of QACS and PMAG-*b*-PMAA, have been successfully prepared under physiological conditions via block ionomer complexes method. The detailed investigations of self-assembly behaviours between PMAG-*b*-PMAA and QACS revealed that both the MW of QACS and titration order could affect the formation of colloidal nanogels. By optimizing the synthesis conditions, glyco/CS-nanogels with compact ionic cross-linked core and glucose corona were obtained and their structure was confirmed by TEM. These nanogels not only showed excellent colloidal stability in 10 mM HEPES buffer solution, but also exhibited specific binding ability to lectin (Con A). Moreover, enhanced polycation-induced cytotoxicity to K562 cells was observed possibly due to the over-expressed GLUT-1 on cell membrane of K562, where the glyco/CS-nanogels exhibited a much higher affinity and cellular internalization. The cellular uptake of these nanogels was further imaged by fluorescent microscopy. After co-incubating K562 and FA-glyco/CS-nanogels for 6 h, the fluorescent nanogels were found to be co-located within the cell nuclei, indicating that the internalized cationic nanogels possibly eventually bound with cell nuclei by electrostatic interactions. The facile preparation, excellent colloidal stability, specific bioactivities, and good imaging ability have made our glyco/CS nanogels a promising candidate for biomedical applications.

Acknowledgements

We acknowledge Prof. Hong Chen, Mr. Zhonglin Lv and Mr. Yuqi Yuan in Soochow University for the assistance in WST-8 assay. This research is financially supported by the National Natural Science Foundation of China (21274124, 21374069, 21174125).

Notes and references

[a] *MOE Key Laboratory of Macromolecular Synthesis and Functionalization, Department of Polymer Science and Engineering, Zhejiang University, Hangzhou 310027, P. R. China. E-mail: lqwang@zju.edu.cn; Fax: +86 571 87952596; Tel: +86 571 87952596*

[b] *Center for Soft Condensed Matter Physics and Interdisciplinary Research, Soochow University, Suzhou, 215006, P. R. China. E-mail: gchen@suda.edu.cn; Fax: +86 512 69155837; Tel: +86 512 65884406*

†Electronic Supplementary Information (ESI) available: Supplementary data, including Fluorescence emission spectra of PMAG-*b*-PMAA and PMAG-*b*-PMAA-FA, DLS and Zeta potential values of diluted glyco/CS-nanogels, and WST-8 assay of K562 cells treated with free QACS 1 and PMAG-*b*-PMAA. See DOI: 10.1039/b000000x/

1. L. L. Kiessling and J. C. Grim, *Chem. Soc. Rev.*, 2013, **42**, 4476-4491.
2. S. N. Narla, H. Nie, Y. Li and X.-L. Sun, *J. Carbohydr. Chem.*, 2012, **31**, 67-92.
3. Y.-C. Yeh, S. T. Kim, R. Tang, B. Yan and V. M. Rotello, *J. Mater. Chem. B*, 2014, **2**, 4610-4614.
4. S. K. Mamidyala, S. Dutta, B. A. Chrunyk, C. Préville, H. Wang, J. M. Withka, A. McColl, T. A. Subashi, S. J. Hawrylik and M. C. Griffor, *J. Am. Chem. Soc.*, 2012, **134**, 1978-1981.
5. G. Yilmaz and C. R. Becer, *Polym. Chem.*, 2015. DOI: 10.1039/C5PY00089K.
6. S. S. Ting, G. Chen and M. H. Stenzel, *Polym. Chem.*, 2010, **1**, 1392-1412.
7. L. Otten, S.-J. Richards, E. Fullam, G. S. Besra and M. I. Gibson, *J. Mater. Chem. B*, 2013, **1**, 2665-2672.
8. X. Li and G. Chen, *Polym. Chem.*, 2015, **6**, 1417-1430.
9. G. Yilmaz and C. R. Becer, *Front. Bioeng. Biotechnol.*, 2014, **2**.
10. M. Ahmed, P. Wattanaarsakit and R. Narain, *Eur. Polym. J.*, 2013, **49**, 3010-3033.
11. X. Li, M. Bao, Y. Weng, K. Yang, W. Zhang and G. Chen, *J. Mater. Chem. B*, 2014, **2**, 5569-5575.
12. J. Lu, W. Zhang, S.-J. Richards, M. I. Gibson and G. Chen, *Polym. Chem.*, 2014, **5**, 2326-2332.
13. J. Lu, W. Zhang, L. Yuan, W. Ma, X. Li, W. Lu, Y. Zhao and G. Chen, *Macromol. Biosci.*, 2014, **14**, 340-346.
14. Z. Deng, S. Li, X. Jiang and R. Narain, *Macromolecules*, 2009, **42**, 6393-6405.
15. W. Lu, W. Ma, J. Lu, X. Li, Y. Zhao and G. Chen, *Macromol. Rapid Commun.*, 2014, **35**, 827-833.
16. C. Boyer, A. Bousquet, J. Rondolo, M. R. Whittaker, M. H. Stenzel and T. P. Davis, *Macromolecules*, 2010, **43**, 3775-3784.

17. W. Chen, F. Meng, R. Cheng, C. Deng, J. Feijen and Z. Zhong, *J. Mater. Chem. B*, 2015, **3**, 2308-2317.
18. S. S. Ting, E. H. Min, P. B. Zetterlund and M. H. Stenzel, *Macromolecules*, 2010, **43**, 5211-5221.
19. M. J. Joralemon, K. S. Murthy, E. E. Remsen, M. L. Becker and K. L. Wooley, *Biomacromolecules*, 2004, **5**, 903-913.
20. X. H. Dai and C. M. Dong, *J. Polym. Sci., Part A: Polym. Chem.*, 2008, **46**, 817-829.
21. X.-H. Dai, C.-M. Dong and D. Yan, *J. Phys. Chem. B*, 2008, **112**, 3644-3652.
22. L. Yin, M. C. Dalsin, A. Sizovs, T. M. Reineke and M. A. Hillmyer, *Macromolecules*, 2012, **45**, 4322-4332.
23. N.-Y. Xiao, A.-L. Li, H. Liang and J. Lu, *Macromolecules*, 2008, **41**, 2374-2380.
24. A. V. Kabanov and S. V. Vinogradov, *Angew. Chem. Int. Ed.*, 2009, **48**, 5418-5429.
25. Y. Terada, W. Hashimoto, T. Endo, H. Seto, T. Murakami, H. Hisamoto, Y. Hoshino and Y. Miura, *J. Mater. Chem. B*, 2014, **2**, 3324-3332.
26. M. Ahmed, P. Wattanaarsakit and R. Narain, *Polym. Chem.*, 2013, **4**, 3829-3836.
27. M. Ahmed and R. Narain, *Molecular pharmaceutics*, 2012, **9**, 3160-3170.
28. R. Sunasee, P. Wattanaarsakit, M. Ahmed, F. B. Lollmahomed and R. Narain, *Bioconjugate Chem.*, 2012, **23**, 1925-1933.
29. M. Ahmed and R. Narain, *Prog. Polym. Sci.*, 2013, **38**, 767-790.
30. Y. Wang, X. Zhang, P. Yu and C. Li, *Int. J. Pharm.*, 2013, **441**, 170-180.
31. S. Shu, X. Zhang, D. Teng, Z. Wang and C. Li, *Carbohydr. Res.*, 2009, **344**, 1197-1204.
32. S. V. Vinogradov, T. K. Bronich and A. V. Kabanov, *Adv. Drug Delivery Rev.*, 2002, **54**, 135-147.
33. Y. Sasaki and K. Akiyoshi, *Chem. Rec.*, 2010, **10**, 366-376.
34. J. O. Kim, N. V. Nukolova, H. S. Oberoi, A. V. Kabanov and T. K. Bronich, *Polym. Sci. Ser. A*, 2009, **51**, 708-718.
35. A. C. Holley, K. H. Parsons, W. Wan, D. F. Lyons, G. R. Bishop, J. J. Correia, F. Huang and C. L. McCormick, *Polym. Chem.*, 2014, **5**, 6967-6976.
36. T. K. Bronich, P. A. Keifer, L. S. Shlyakhtenko and A. V. Kabanov, *J. Am. Chem. Soc.*, 2005, **127**, 8236-8237.
37. K. Kataoka, H. Togawa, A. Harada, K. Yasugi, T. Matsumoto and S. Katayose, *Macromolecules*, 1996, **29**, 8556-8557.
38. A. V. Kabanov and V. A. Kabanov, *Adv. Drug Delivery Rev.*, 1998, **30**, 49-60.
39. A. J. Keefe and S. Jiang, *Nat Chem*, 2012, **4**, 59-63.
40. M. C. Deshpande, M. C. Davies, M. C. Garnett, P. M. Williams, D. Armitage, L. Bailey, M. Vamvakaki, S. P. Armes and S. Stolnik, *J. Control. Release*, 2004, **97**, 143-156.
41. S. Mishra, P. Webster and M. E. Davis, *Eur. J. Cell Biol.*, 2004, **83**, 97-111.
42. L. Song, Q. Ahkong, Q. Rong, Z. Wang, S. Ansell, M. Hope and B. Mui, *BBA-Biomembranes*, 2002, **1558**, 1-13.
43. C. S. Fishburn, *J. Pharm. Sci.*, 2008, **97**, 4167-4183.
44. F. M. Veronese, *Biomaterials*, 2001, **22**, 405-417.
45. Z. Deng, M. Ahmed and R. Narain, *J. Polym. Sci., Part A: Polym. Chem.*, 2009, **47**, 614-627.
46. I. Kurtulus, G. Yilmaz, M. Ucuncu, M. Emrullahoglu, C. R. Becer and V. Bulmus, *Polym. Chem.*, 2014, **5**, 1593-1604.
47. L. Szablewski, *BBA-Rev. Cancer*, 2013, **1835**, 164-169.
48. M. Younes, L. V. Lechago, J. R. Somoano, M. Mosharaf and J. Lechago, *Cancer Res*, 1996, **56**, 1164-1167.
49. M. L. Macheda, S. Rogers and J. D. Best, *J. Cell. Physiol.*, 2005, **202**, 654-662.
50. N. Suganuma, F. Segade, K. Matsuzu and D. W. Bowden, *BJU Int.*, 2007, **99**, 1143-1149.
51. F. Yuan, S. Wang, G. Chen, K. Tu, H. Jiang and L.-Q. Wang, *Colloid Surf. B-Biointerfaces*, 2014, **122**, 194-201.
52. Z. Zhang, X. Zhu, J. Zhu, Z. Cheng and S. Zhu, *J. Polym. Sci., Part A: Polym. Chem.*, 2006, **44**, 3343-3354.
53. M. R. Whittaker, Y.-K. Goh, H. Gemici, T. M. Legge, S. Perrier and M. J. Monteiro, *Macromolecules*, 2006, **39**, 9028-9034.
54. J. W. Chan, C. E. Hoyle, A. B. Lowe and M. Bowman, *Macromolecules*, 2010, **43**, 6381-6388.
55. G. Chen, S. Amajjahe and M. H. Stenzel, *Chem. Commun.*, 2009, 1198-1200.
56. E. K. Cloherty, D. L. Diamond, K. S. Heard and A. Carruthers, *Biochemistry*, 1996, **35**, 13231-13239.
57. N. Ahmed and M. V. Berridge, *Leuk. Res.*, 1999, **23**, 395-401.
58. R. A. Medina and G. I. Owen, *Biol. Res.*, 2002, **35**, 9-26.

TOC：

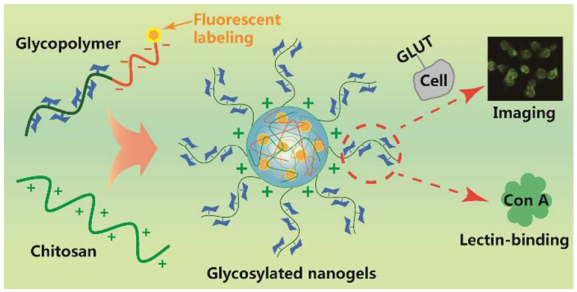

Glycosylated polyelectrolyte nanogels from natural and synthetic sugar polymers with excellent colloidal stability, specific bioactivities and imaging ability.